École Doctorale des Sciences de l'Environnement d'Île-de-France

Année Universitaire 2015-2016

Modélisation Numérique de l'Écoulement Atmosphérique et Assimilation de Données

Olivier Talagrand

Cours 2

30 Mars 2016

Lois physiques régissant l’écoulement

- Conservation de la masse

  $D\rho/Dt + \rho \,\mathrm{div}\underline{U} = 0$

- Conservation de l’énergie

  $De/Dt - (p/\rho^2)\, D\rho/Dt = Q$

- Conservation de la quantité de mouvement

  $D\underline{U}/Dt + (1/\rho)\, \underline{\mathrm{grad}p} - \underline{g} + 2\, \underline{\Omega} \wedge \underline{U} = \underline{F}$

- Equation d’état

  $f(p, \rho, e) = 0$ $(p/\rho = rT,\ e = C_v T)$

- Conservation de la masse de composants secondaires (eau pour l’atmosphère, sel pour l’océan, espèces chimiques, …)

  $Dq/Dt + q\, \mathrm{div}\underline{U} = S$

Lois physiques doivent en pratique être discrétisées dans le temps et dans l'espace $\Rightarrow$ *modèles numériques*, nécessairement imparfaits.

Les modèles utilisés pour la prévision météorologique de grande échelle et la simulation climatologique couvrent la totalité du volume de l'atmosphère. Ils sont, jusqu'à présent au moins, construits sur l'hypothèse *hydrostatique*

Dans la direction verticale :

$$\partial p/\partial z + \rho g = 0$$

Élimine l'équation du mouvement pour la direction verticale; en outre, l'écoulement est incompressible dans les coordonnées (x, y, p) $\Rightarrow$ nombre d'équations pronostiques diminué de deux unités.

Approximation hydrostatique valide pour échelles horizontales > 20-30 km

Modèles non-hydrostatiques, plus coûteux, sont utilisés pour la météorologie de petite échelle.

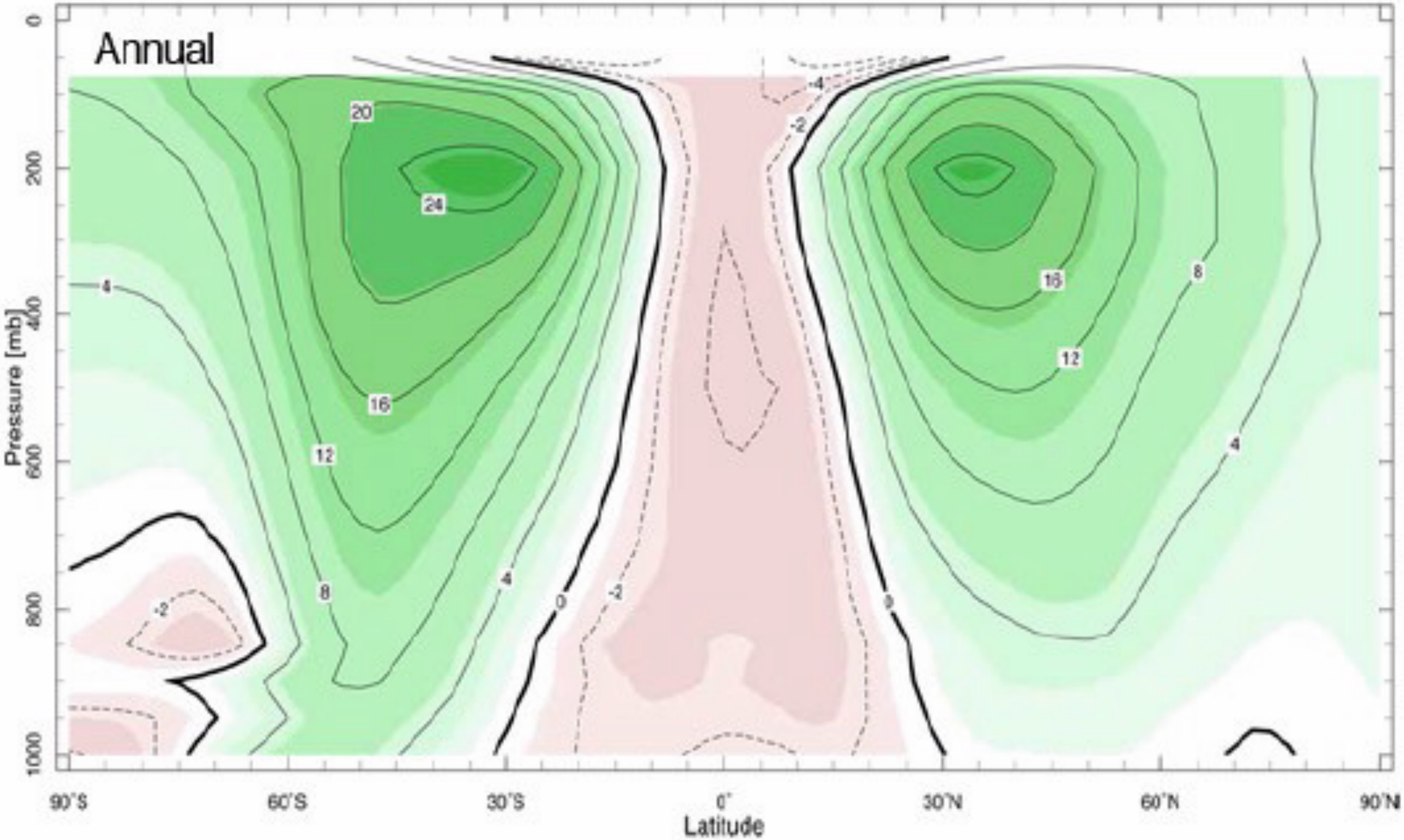

Vent zonal; moyenne longitudinale annuelle ($m.s^{-1}$)
http://paoc.mit.edu/labweb/notes/chap5.pdf,
Atmosphere, Ocean and Climate Dynamics, by J. Marshall and R. A. Plumb,
International Geophysics, Elsevier)

In addition to hydrostatic approximation, the following approximations are (almost) systematically made in global modeling :

- Atmospheric fluid is contained in a spherical shell with negligible thickness. This does not forbid the existence within the shell of a vertical coordinate which, in view of the hydrostatic equation, can be chosen as the pressure p.

- The horizontal component of the Coriolis acceleration due to the vertical motion is neglected (this approximation, sometimes called the *traditional approximation*, is actually a consequence of the previous one).

- Tidal forces are neglected.

These approximations lead to the so-called (and ill-named) *primitive equations*

Pressure p, although convenient for writing down the equations, is in fact rather inconvenient because lower boundary is not fixed in (x, y, p)-space.

So-called σ-coordinate. $\sigma \equiv p/p_S$, where p_S is pressure at ground level.

'Hybrid' coordinate.

Lois physiques régissant l'écoulement

- Conservation de la masse

  $D\rho/Dt + \rho \, \mathrm{div}\underline{U} = 0$

- Conservation de l'énergie

  $De/Dt - (p/\rho^2)\, D\rho/Dt = Q$

- Conservation de la quantité de mouvement

  $D\underline{U}/Dt + (1/\rho)\, \underline{\mathrm{grad}p} - \underline{g} + 2\, \underline{\Omega} \wedge \underline{U} = \underline{F}$

- Equation d'état

  $f(p, \rho, e) = 0$ $(p/\rho = rT,\ e = C_v T)$

- Conservation de la masse de composants secondaires (eau pour l'atmosphère, sel pour l'océan, espèces chimiques, …)

  $Dq/Dt + q \, \mathrm{div}\underline{U} = S$

Temporal discretization. Courant-Friedrichs-Lewy (CFL) condition for stability of explicit schemes

$$\Delta t \,/\, \Delta x \; < \alpha \,/\, c$$

where c is phase velocity of fastest propagating (wave) in the system, and α is an $O(1)$ numerical coefficient depending on particular scheme under consideration.

Significance : numerical propagation of signal must be at least as fast as physical propagation.

In hydrostatic atmosphere, fastest propagating wave : gravity wave with largest scale height, $c = \sqrt{(rT)} \approx 300$ m.s^{-1}.

$$\Delta x = 30 \text{ km} \qquad \Rightarrow \; \Delta t = 100 \text{ s}$$

The use of *semi-implicit* schemes allows to get rid of the CFL condition, and to use longer timesteps.

In the parlance of the trade, one distinguishes two different parts in models. The ‘dynamics’ deals with the physically reversible processes (pressure forces, Coriolis force, advection, …), while the ‘physics’ deals with physically irreversible processes, in particular the diabatic heating term Q in the energy equation, and also the parameterization of subgrid scales effects.

Numerical schemes have been gradually developed and validated for the ‘dynamics’ component of models, which are by and large considered now to work satisfactorily (although regular improvements are still being made; project *DYNAMICO*, *Dynamical Core on Icosahedral Grid*, Th. Dubos, IPSL).

The situation is different as concerns ‘physics’, where many problems remain (as concerns for instance subgrid scales parameterization, the water cycle and the associated exchanges of energy, or the exchanges that take place in the boundary layer between the atmosphere and the underlying medium). ‘Physics’ as a whole remains the weaker point of models, and is still the object of active research.

5 - SCHEMA DES INTERACTIONS PHYSIQUES DANS LE MODELE

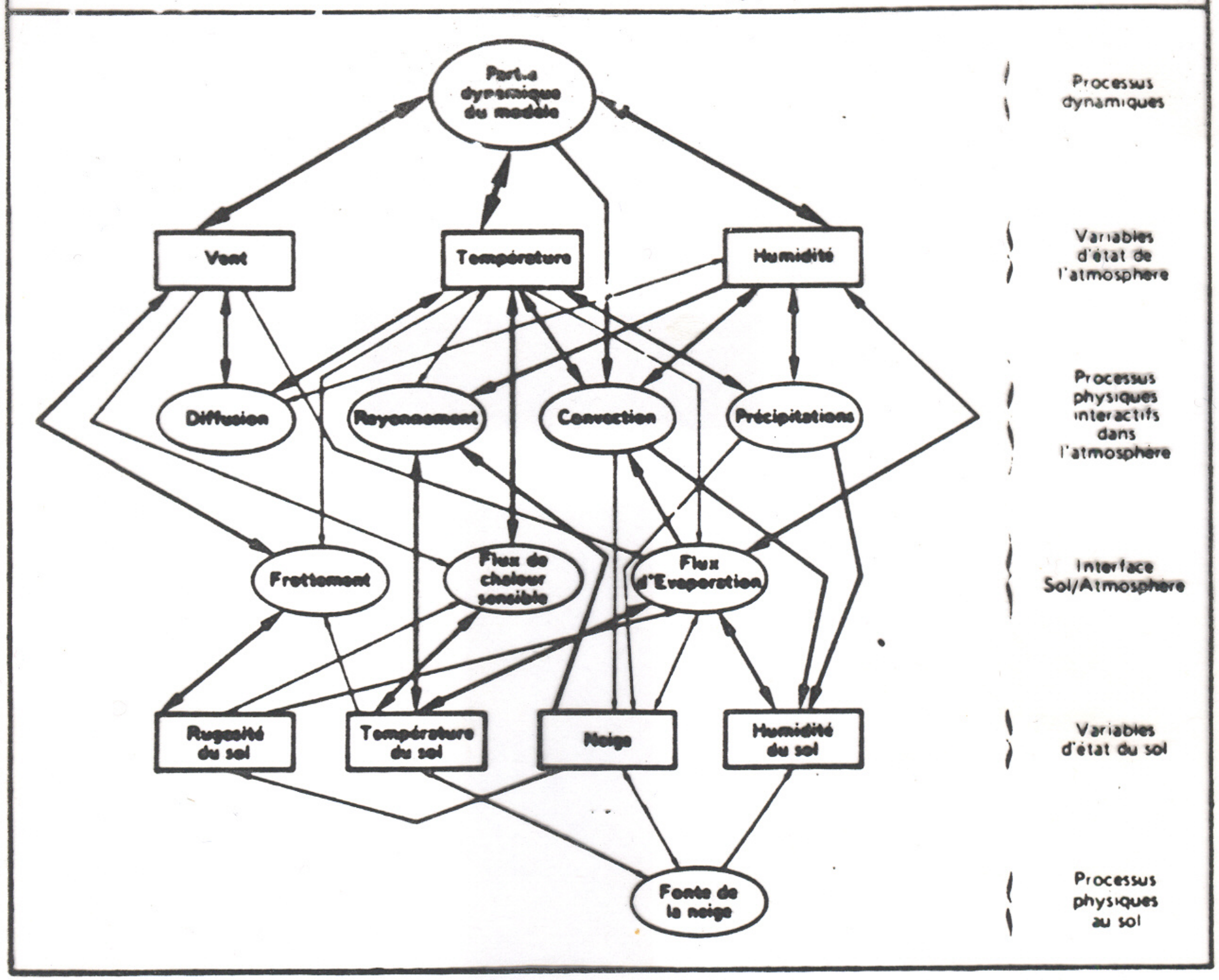

Centre Européen pour les Prévisions Météorologiques à Moyen Terme (CEPMMT, Reading, GB)

(European Centre for Medium-range Weather Forecasts, ECMWF)

Depuis juin 2013 :

Troncature triangulaire T1279 (résolution horizontale ≈ 16 kilomètres)

137 niveaux dans la direction verticale (0 - 80 km)

Dimension du vecteur d'état correspondant ≈ 2,3 10^9

Pas de discrétisation temporelle (schéma semi-Lagrangien semi-implicite): 10 minutes

Sunday 10 January 2016 00UTC ©ECMWF Forecast t+168 VT: Sunday 17 January 2016 00UTC
850 hPa Temperature / 500 hPa Geopotential

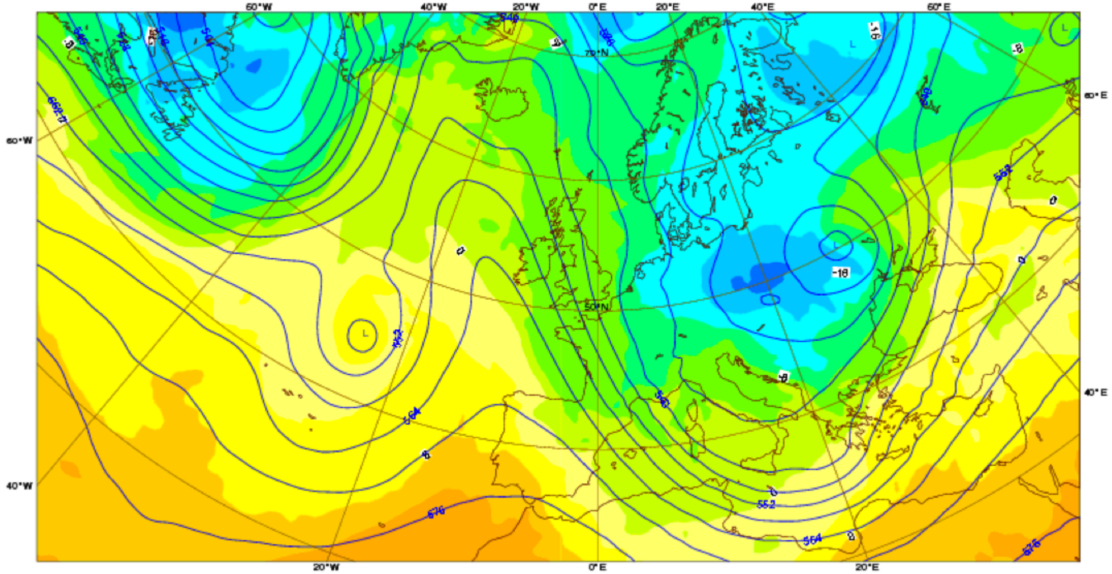

Sunday 17 January 2016 00UTC ©ECMWF Analysis t+000 VT: Sunday 17 January 2016 00UTC
850 hPa Temperature / 500 hPa Geopotential

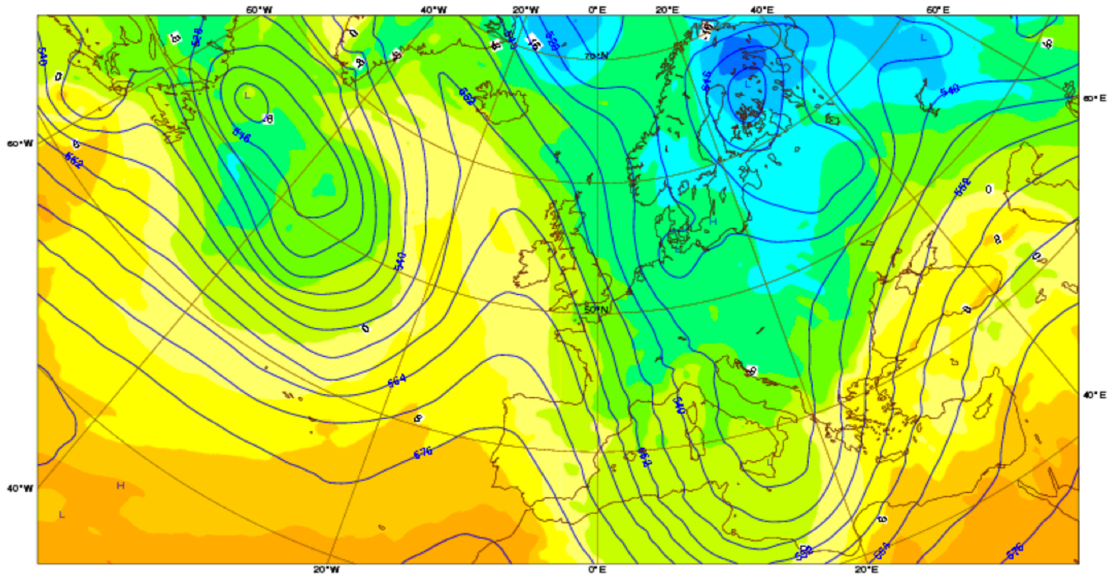

Sunday 10 January 2016 00UTC ©ECMWF Analysis t+000 VT: Sunday 10 January 2016 00UTC
850 hPa Temperature / 500 hPa Geopotential

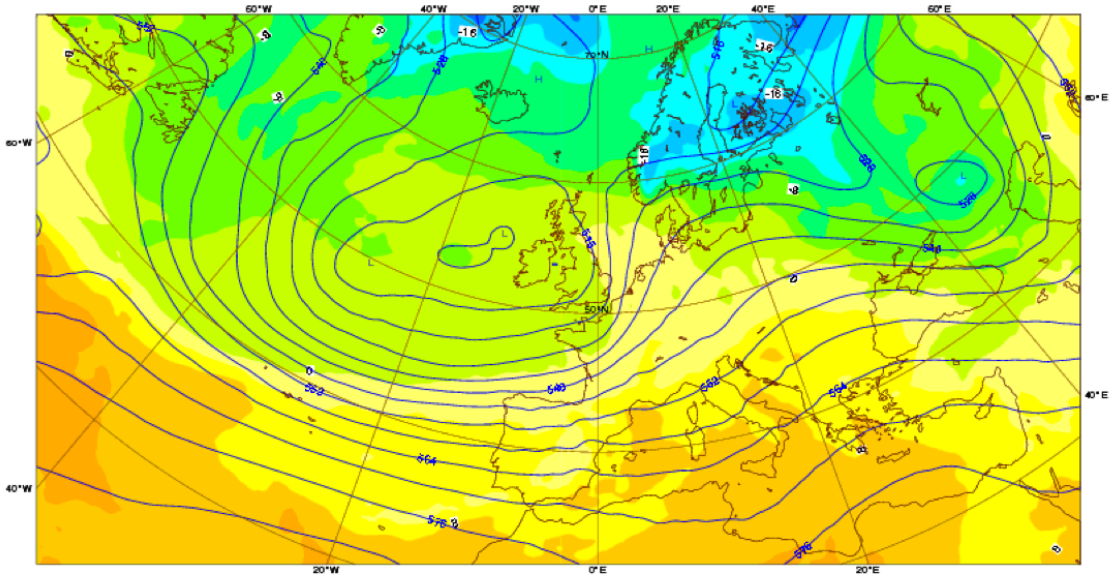

Sunday 17 January 2016 00UTC ©ECMWF Analysis t+000 VT: Sunday 17 January 2016 00UTC
850 hPa Temperature / 500 hPa Geopotential

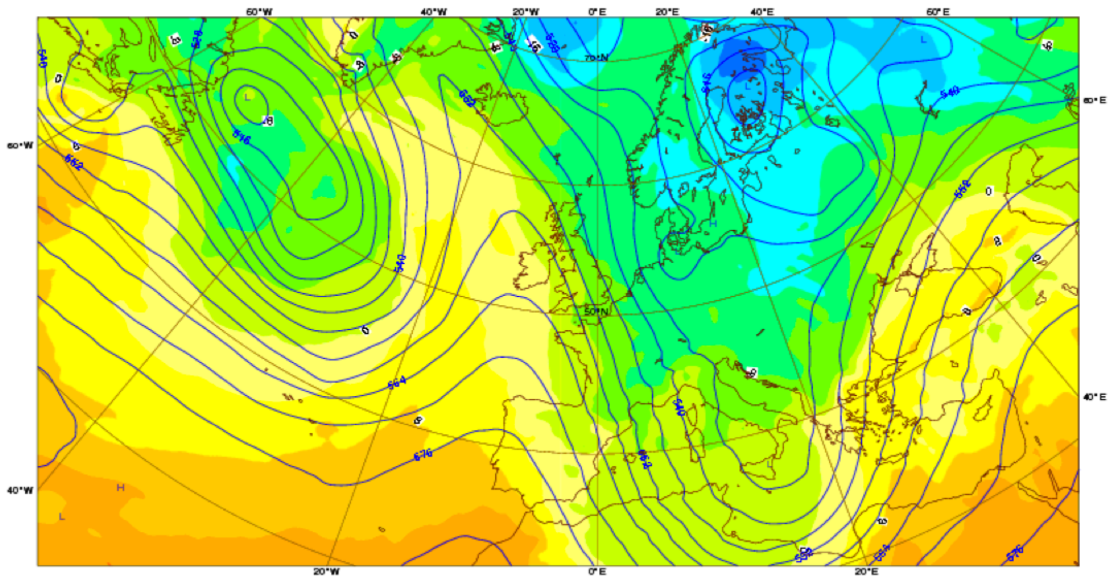

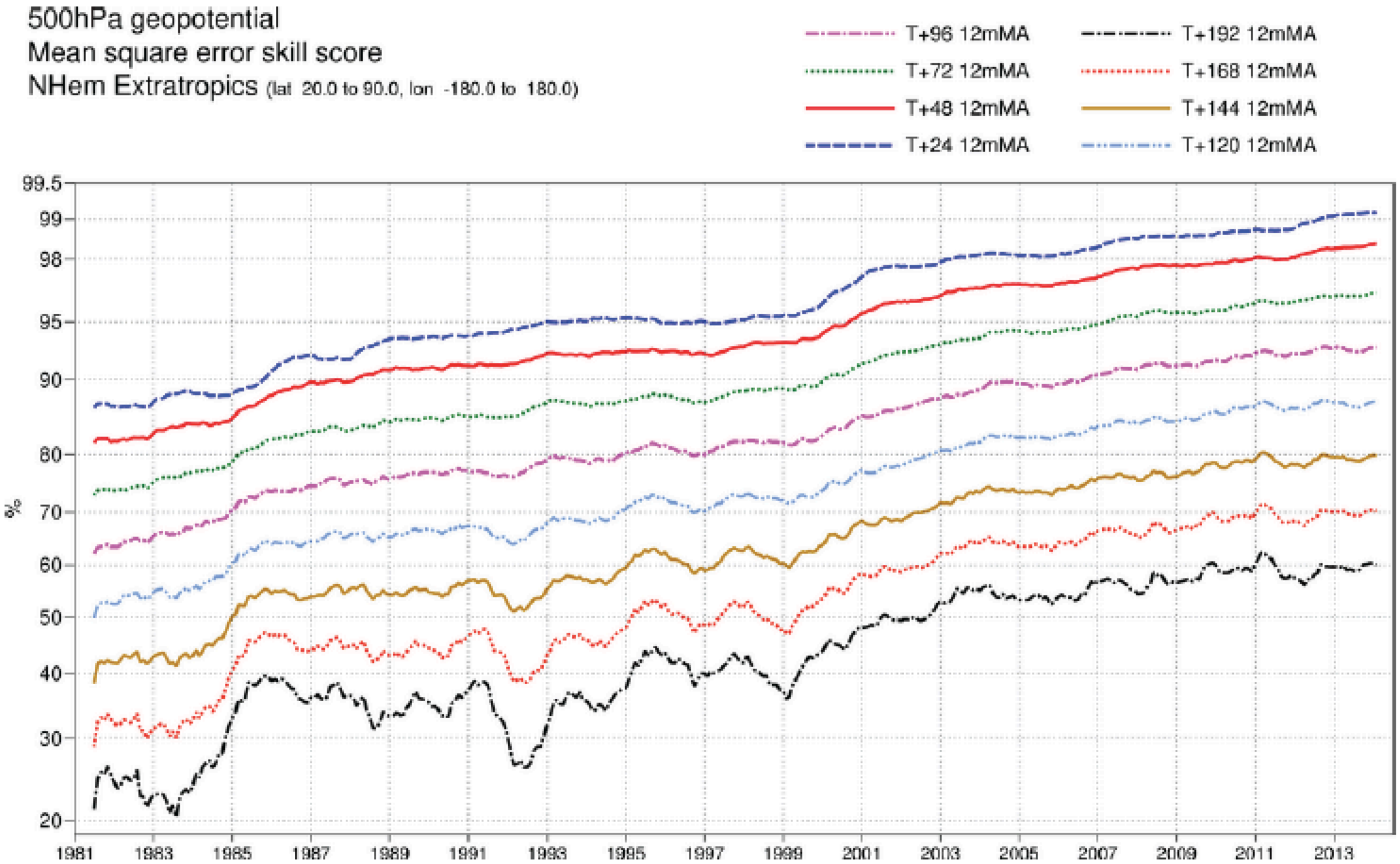

Figure 3: 500 hPa geopotential height mean square error skill score for Europe (top) and the northern hemisphere extratropics (bottom), showing 12-month moving averages for forecast ranges from 24 to 192 hours. The last point on each curve is for the 12-month period August 2013–July 2014.

Persistence = 0 ; climatology = 50 at long range

Initial state error reduction

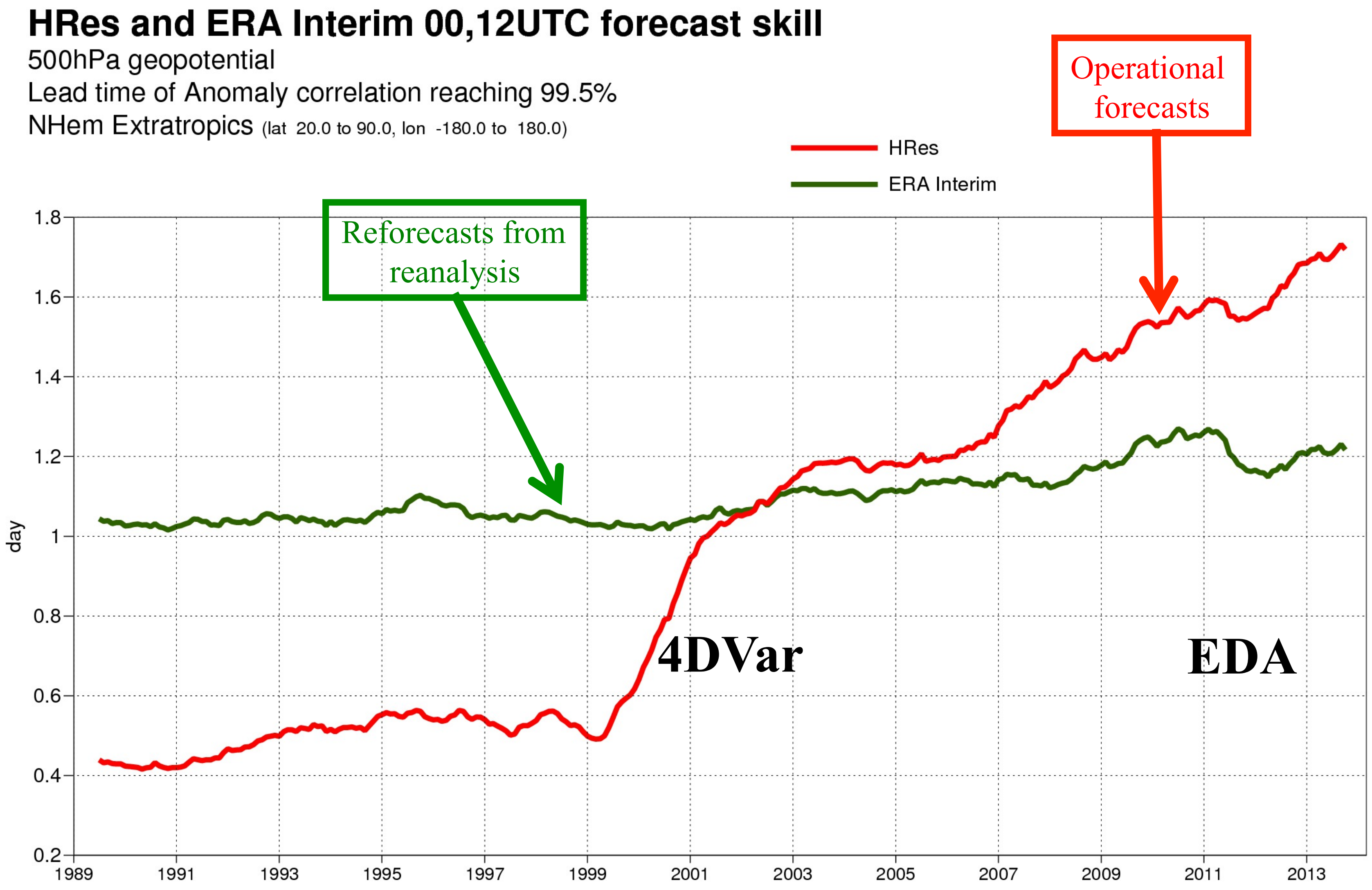

Credit E. Källén, ECMWF

Résultats extraits de :

Haiden *et al.*, 2015,, *Evaluations of ECMWF forecasts including 2014-2015 upgrades,* Memorandum Technique 765, CEPMMT, Reading, GB.

Disponible à l'adresse

http://www.ecmwf.int/sites/default/files/elibrary/2015/15275-evaluation-ecmwf-forecasts-including-2014-2015-upgrades.pdf

(voir aussi l'ensemble du site du CEPMMT)

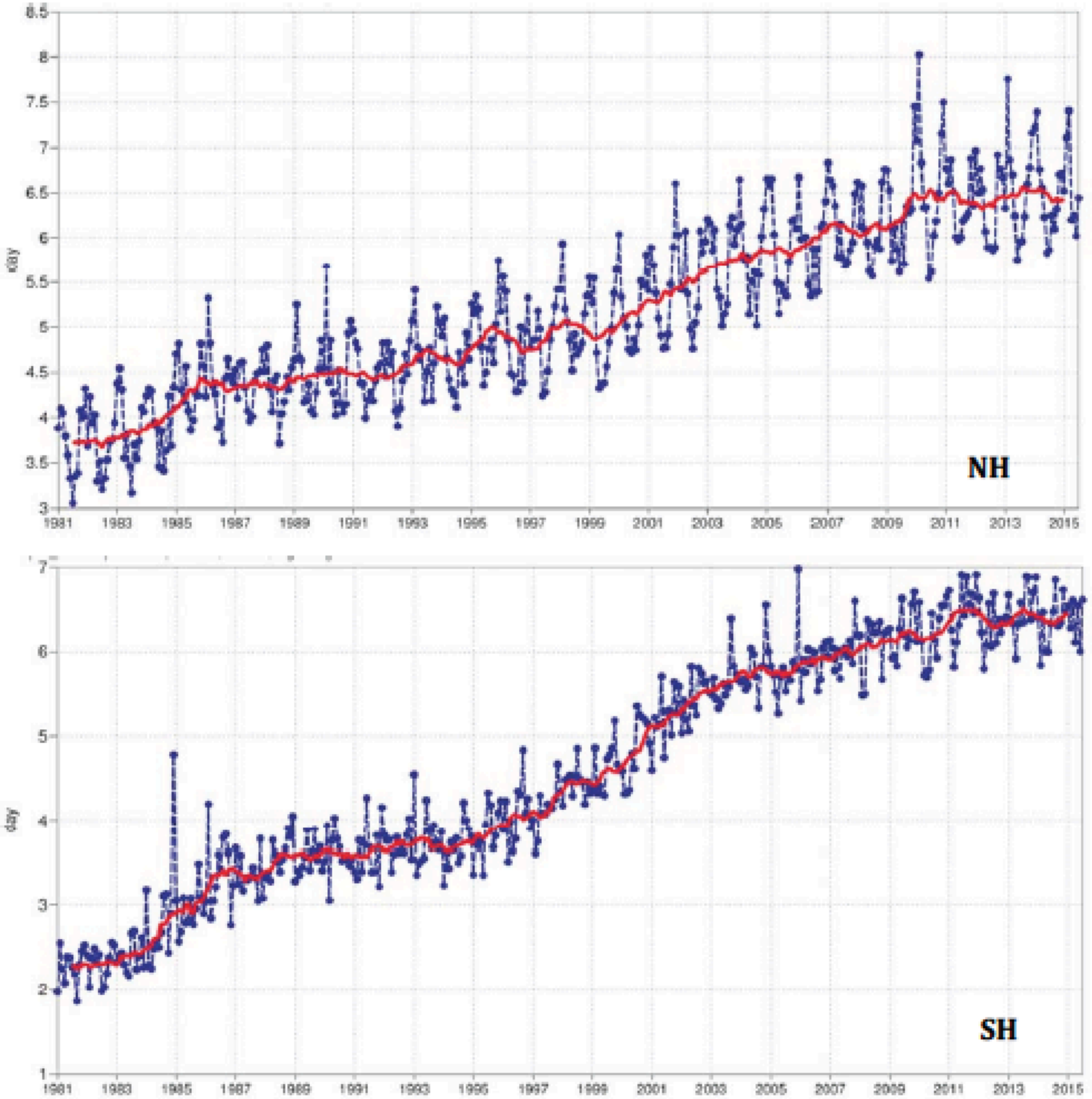

Figure 2: Primary headline score for the high-resolution forecasts. Evolution with time of the 500 hPa geopotential height forecast performance – each point on the curves is the forecast range at which the monthly mean (blue lines) or 12-month mean centred on that month (red line) of the forecast anomaly correlation (ACC) with the verifying analysis falls below 80% for Europe (top), northern hemisphere extratropics (centre) and southern hemisphere extratropics (bottom).

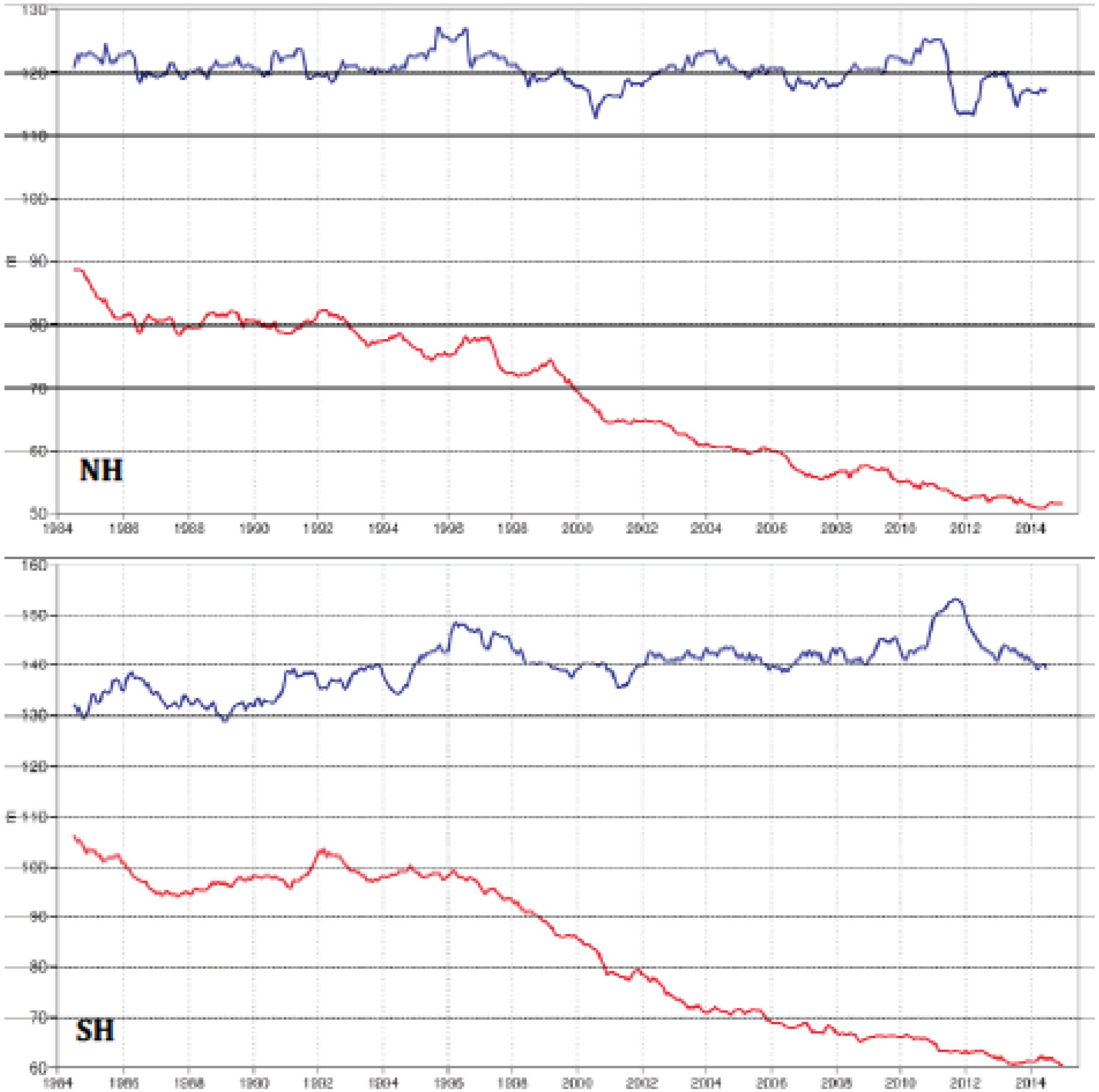

Figure 3: Root mean square (RMS) error of forecasts of 500 hPa geopotential height (m) at day 6 (red), verified against analysis. For comparison, a reference forecast made by persisting the analysis over 6 days is shown (blue). Plotted values are 12-month moving averages; the last point on the curves is for the 12-month period August 2014–July 2015. Results are shown for the northern extra-tropics (top), and the southern extra-tropics (bottom).

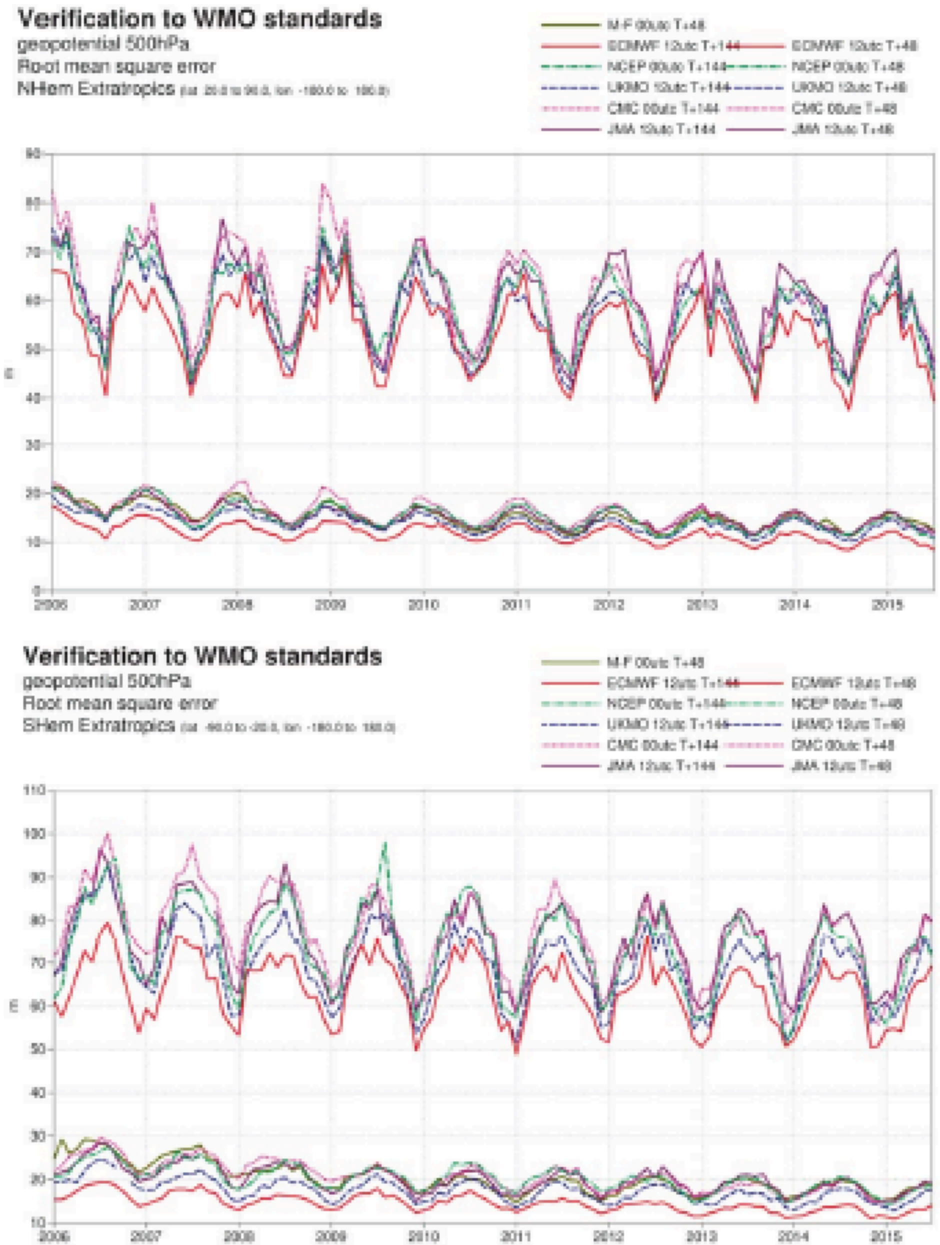

Figure 13: WMO-exchanged scores from global forecast centres. RMS error of 500 hPa geopotential height over northern (top) and southern (bottom) extratropics. In each panel the upper curves show the six-day forecast error and the lower curves show the two-day forecast error. Each model is verified against its own analysis. JMA = Japan Meteorological Agency, CMC = Canadian Meteorological Centre, UKMO = the UK Met Office, NCEP = U.S. National Centers for Environmental Prediction, M-F = Météo France.

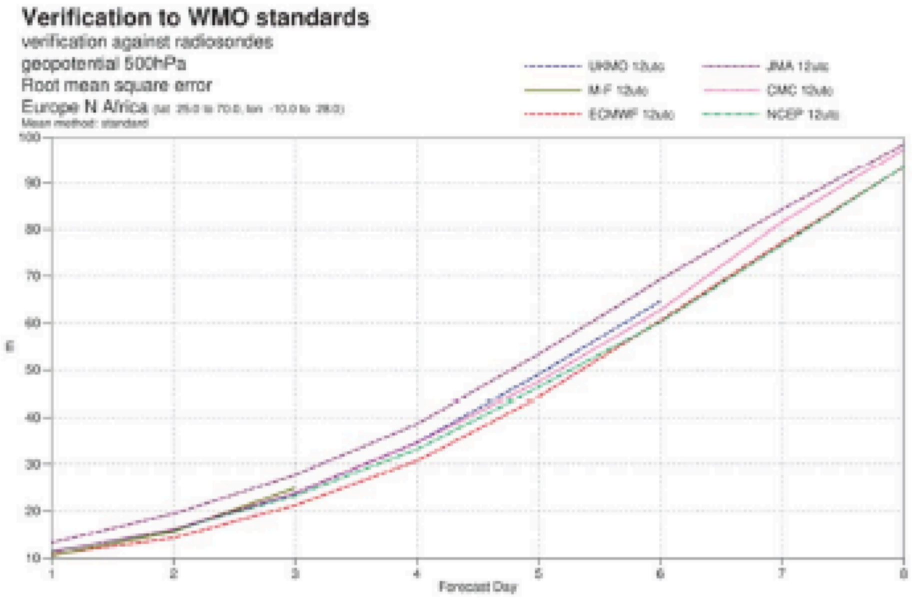

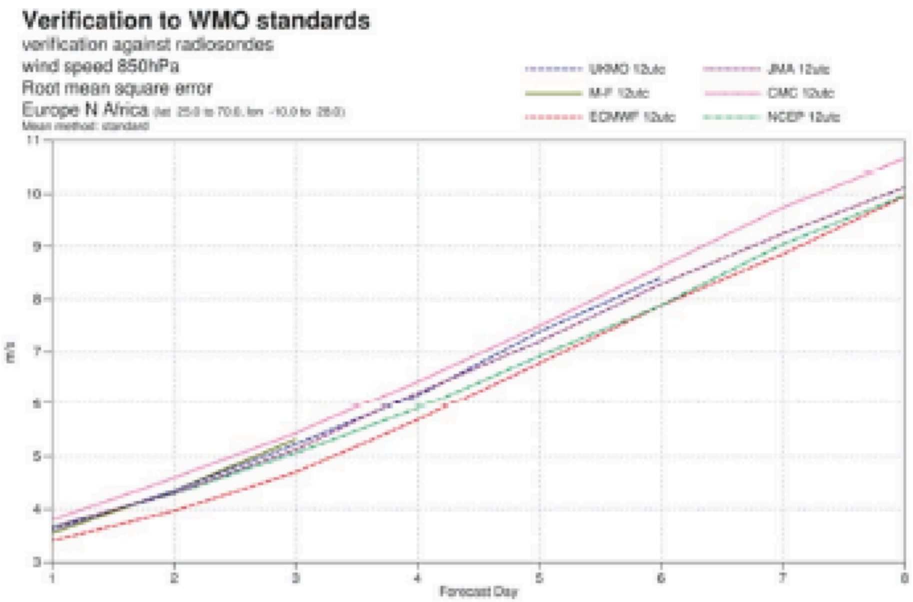

Figure 14: WMO-exchanged scores for verification against radiosondes: 500 hPa height (top) and 850 hPa wind (bottom) RMS error over Europe (annual mean August 2014–July 2015).

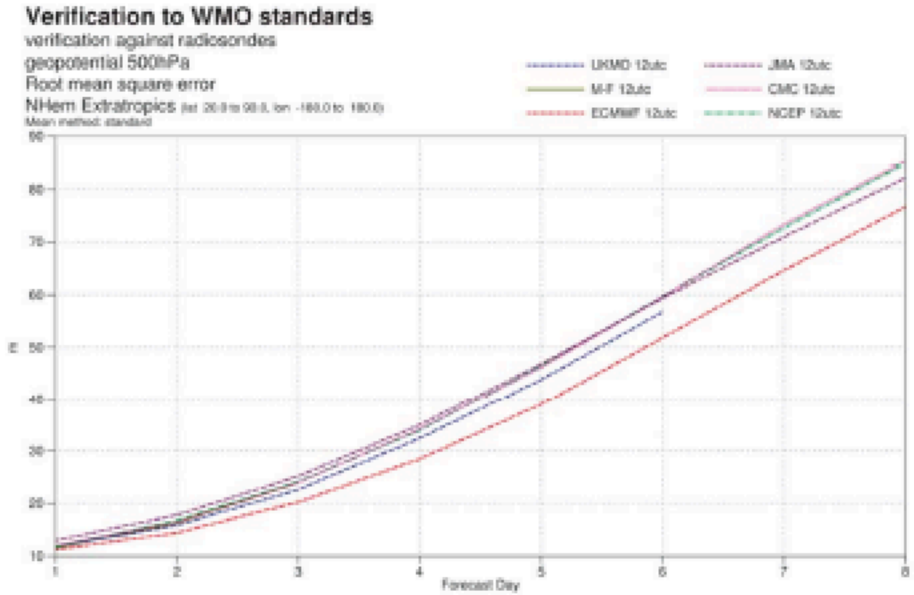

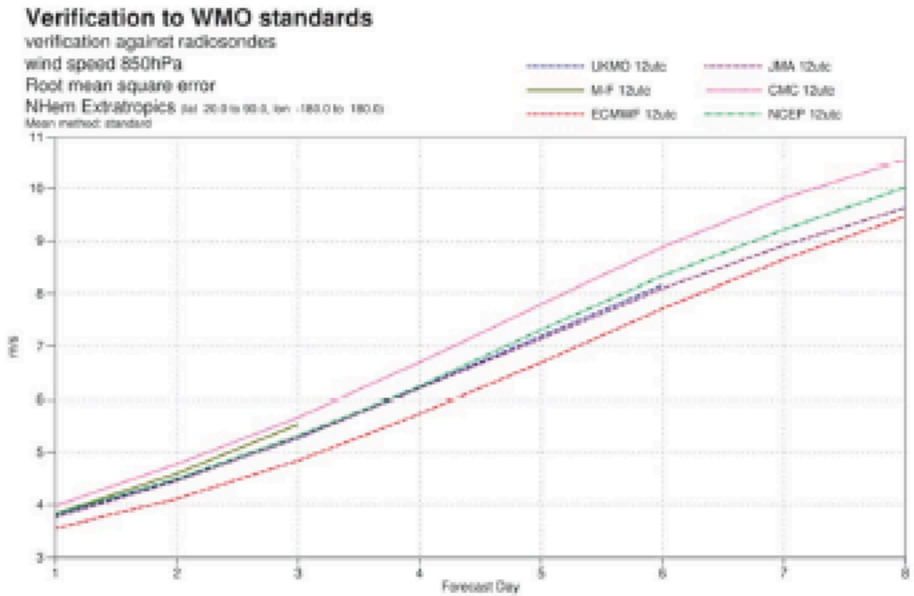

Figure 15: As Figure 14 for the northern hemisphere extratropics.

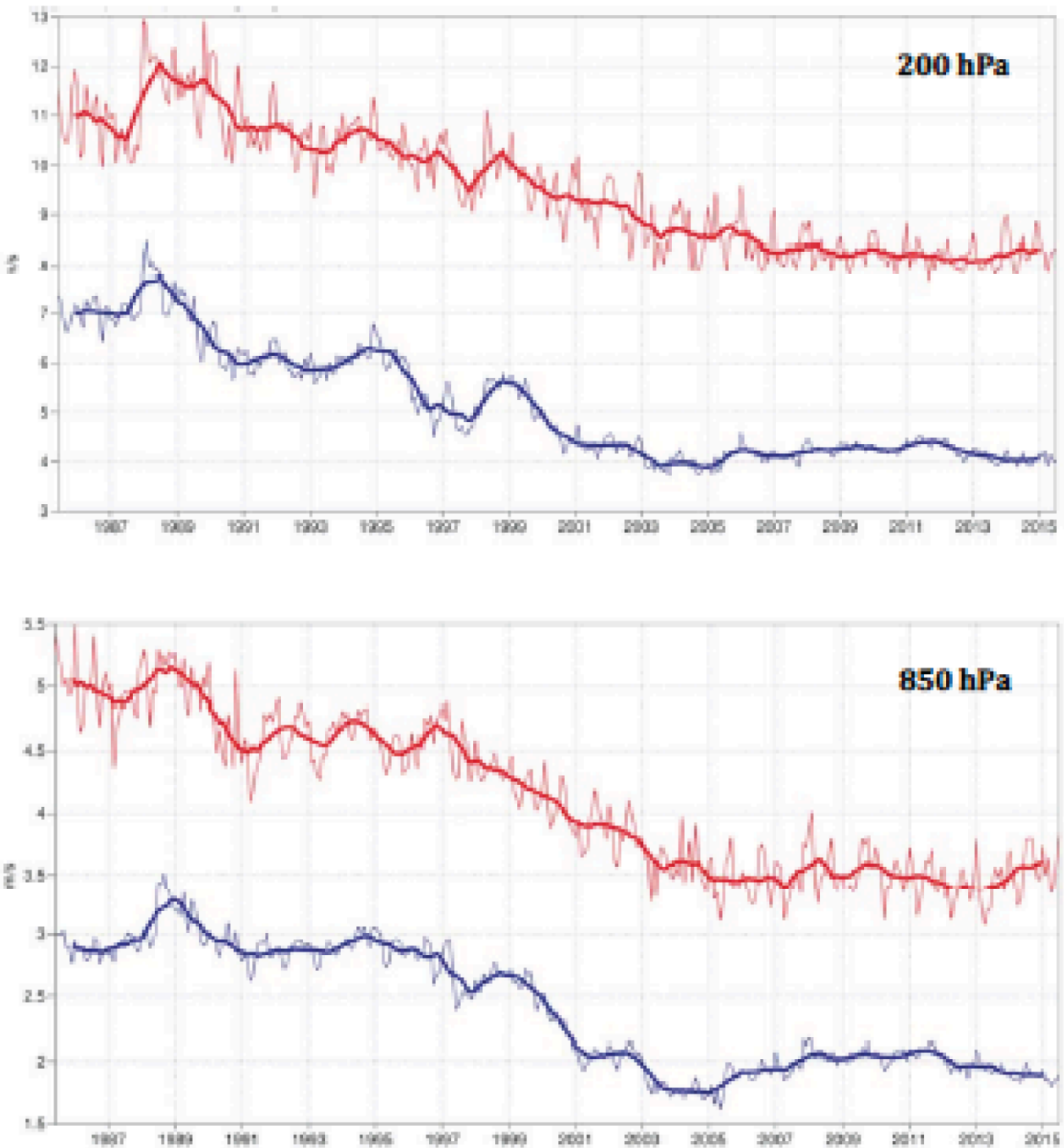

Figure 12: Forecast performance in the tropics. Curves show the monthly average RMS vector wind errors at 200 hPa (top) and 850 hPa (bottom) for one-day (blue) and five-day (red) forecasts, verified against analysis. 12-month moving average scores are also shown (in bold).

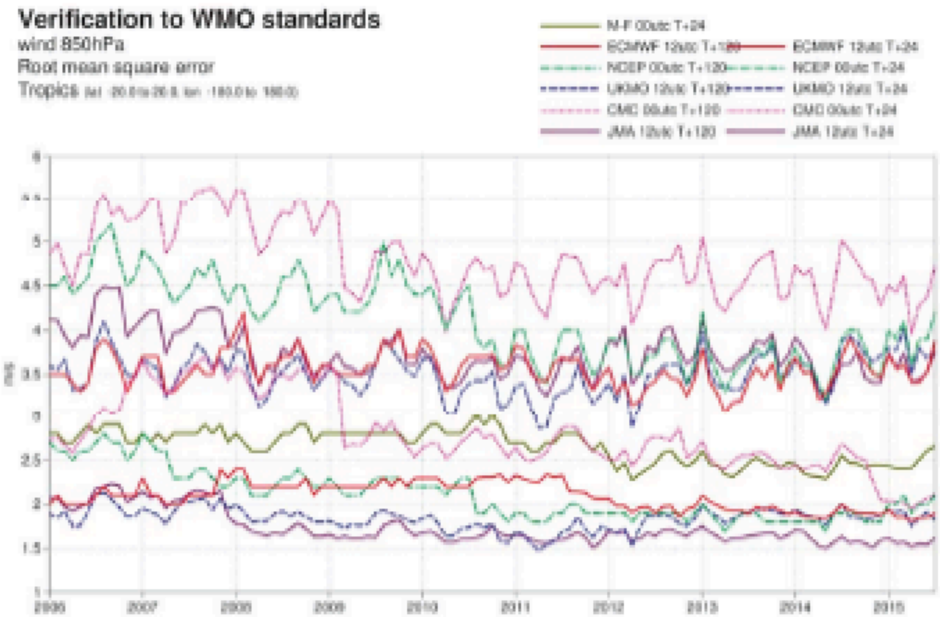

Figure 16: WMO-exchanged scores from global forecast centres. RMS vector wind error over tropics at 250 hPa (top) and 850 hPa (bottom). In each panel the upper curves show the five-day forecast error and the lower curves show the one-day forecast error. Each model is verified against its own analysis.

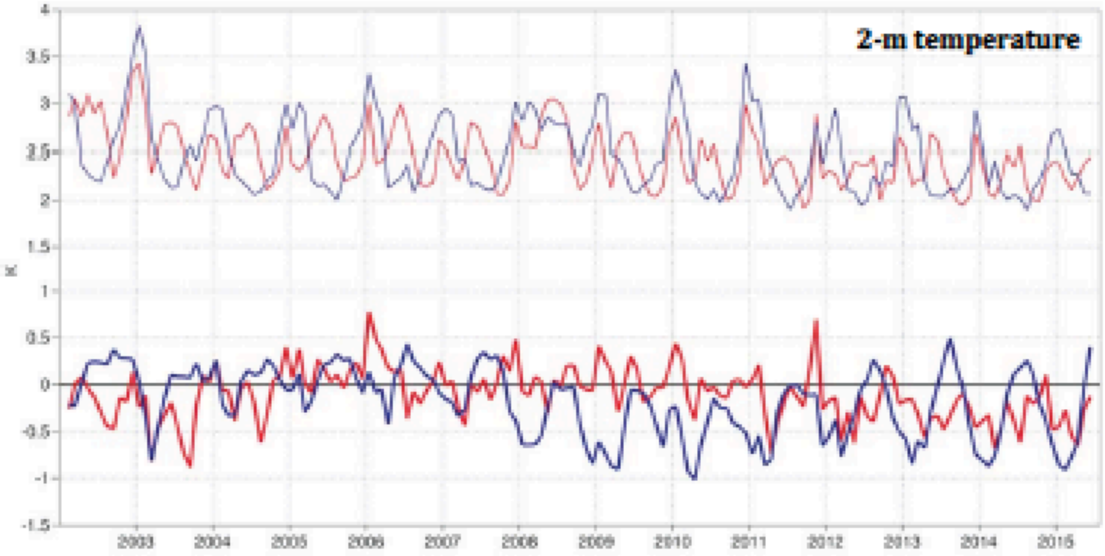

Figure 20: Verification of 2 m temperature forecasts against European SYNOP data on the GTS for 60-hour (night-time) and 72-hour (daytime) forecasts. Lower pair of curves shows bias, upper curves are standard deviation of error.

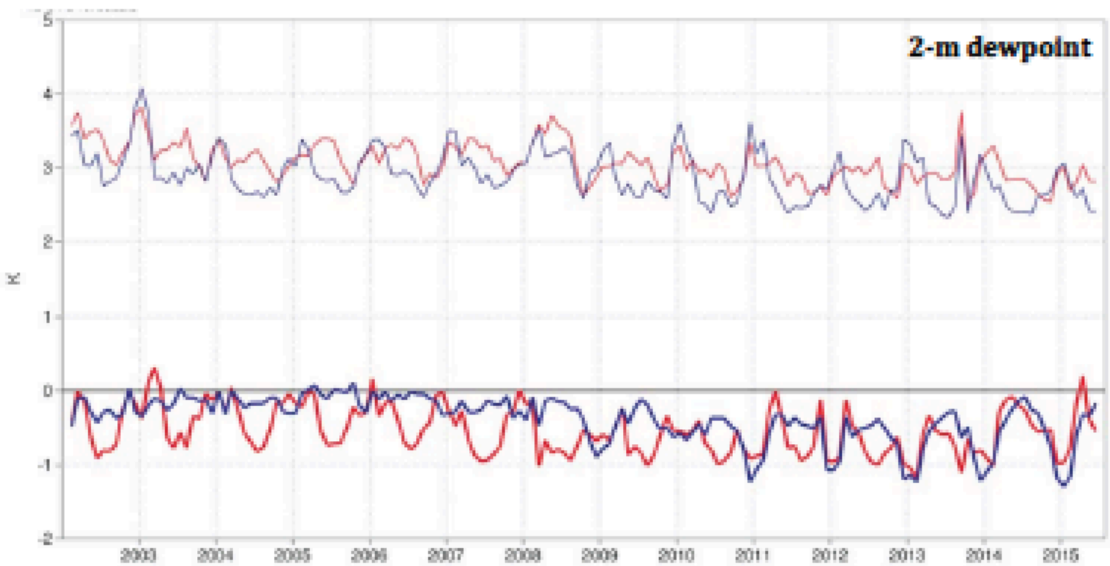

Figure 21: Verification of 2 m dewpoint forecasts against European SYNOP data on the Global Telecommunication System (GTS) for 60-hour (night-time) and 72-hour (daytime) forecasts. Lower pair of curves shows bias, upper curves show standard deviation of error.

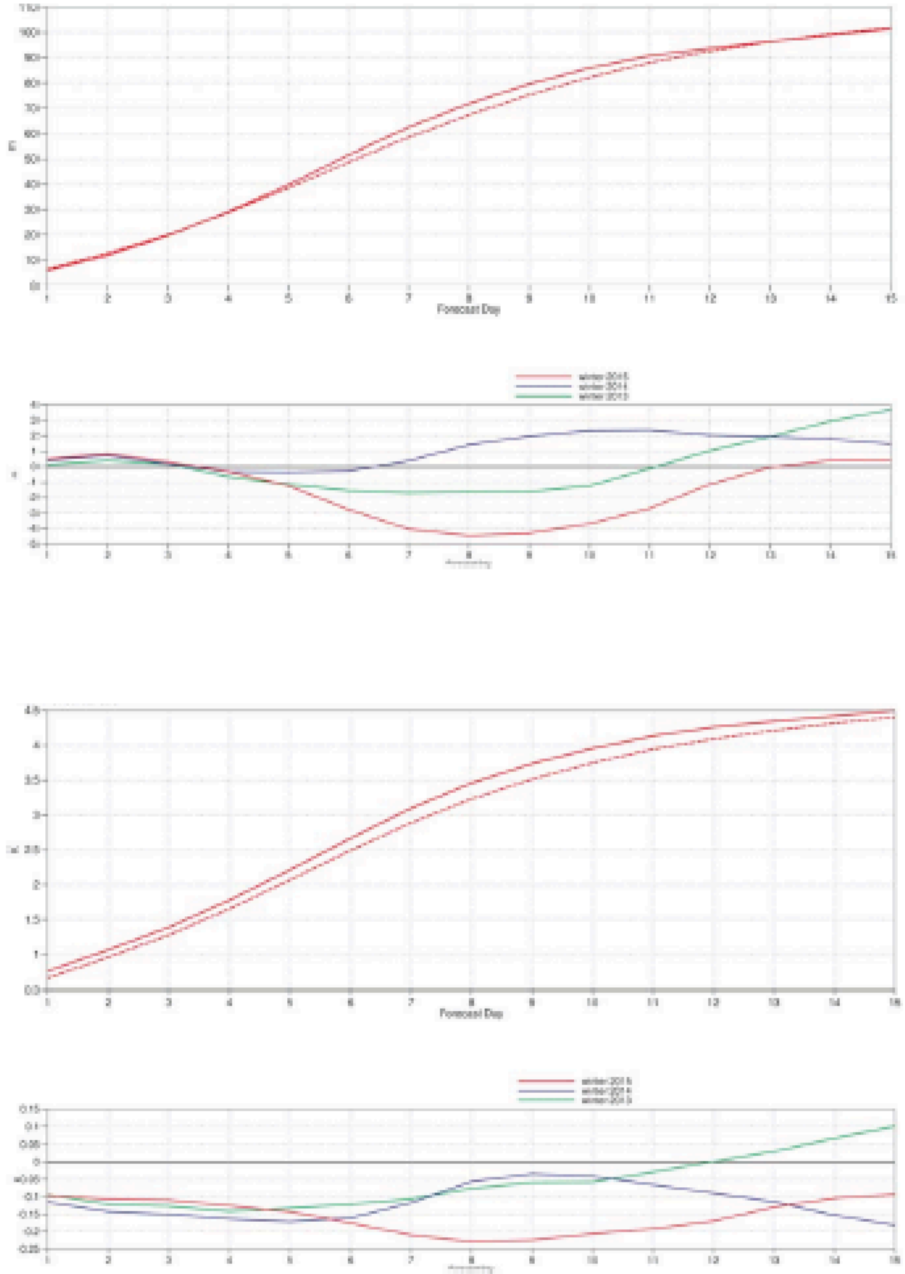

Figure 8: Ensemble spread (standard deviation, dashed lines) and RMS error of ensemble-mean (solid lines) for winter 2014–2015 (upper figure in each panel), and differences of ensemble spread and RMS error of ensemble mean for last three winter seasons (lower figure in each panel, negative values indicate spread is too small); verification is against analysis, plots are for 500 hPa geopotential (top) and 850 hPa temperature (bottom) over the extratropical northern hemisphere for forecast days 1 to 15.

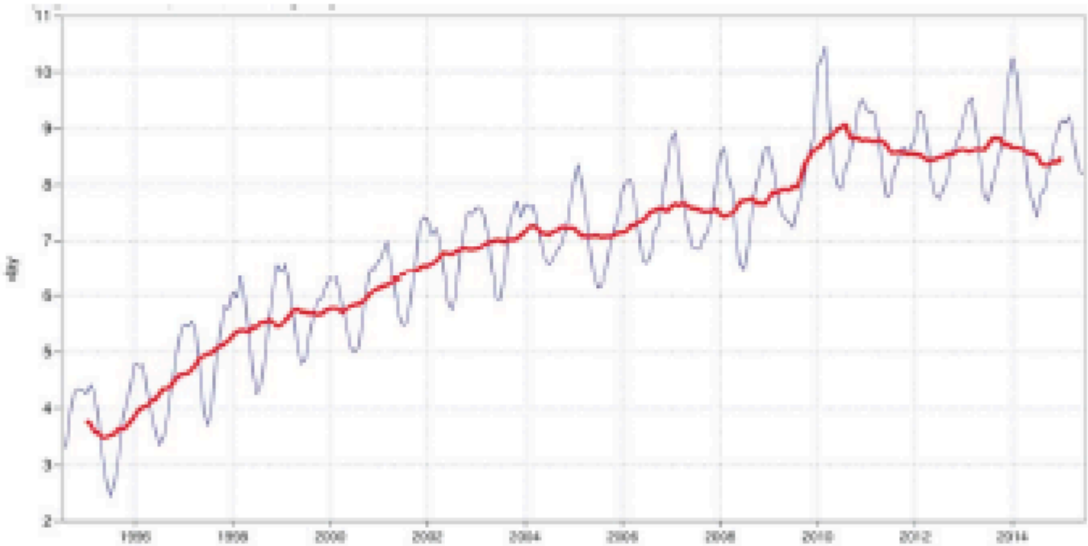

Figure 7: Primary headline score for the ensemble probabilistic forecasts. Evolution with time of 850 hPa temperature ensemble forecast performance, verified against analysis. Each point on the curves is the forecast range at which the 3-month mean (blue lines) or 12-month mean centred on that month (red line) of the continuous ranked probability skill score (CPRSS) falls below 25% for Europe (top), northern hemisphere extratropics (bottom).

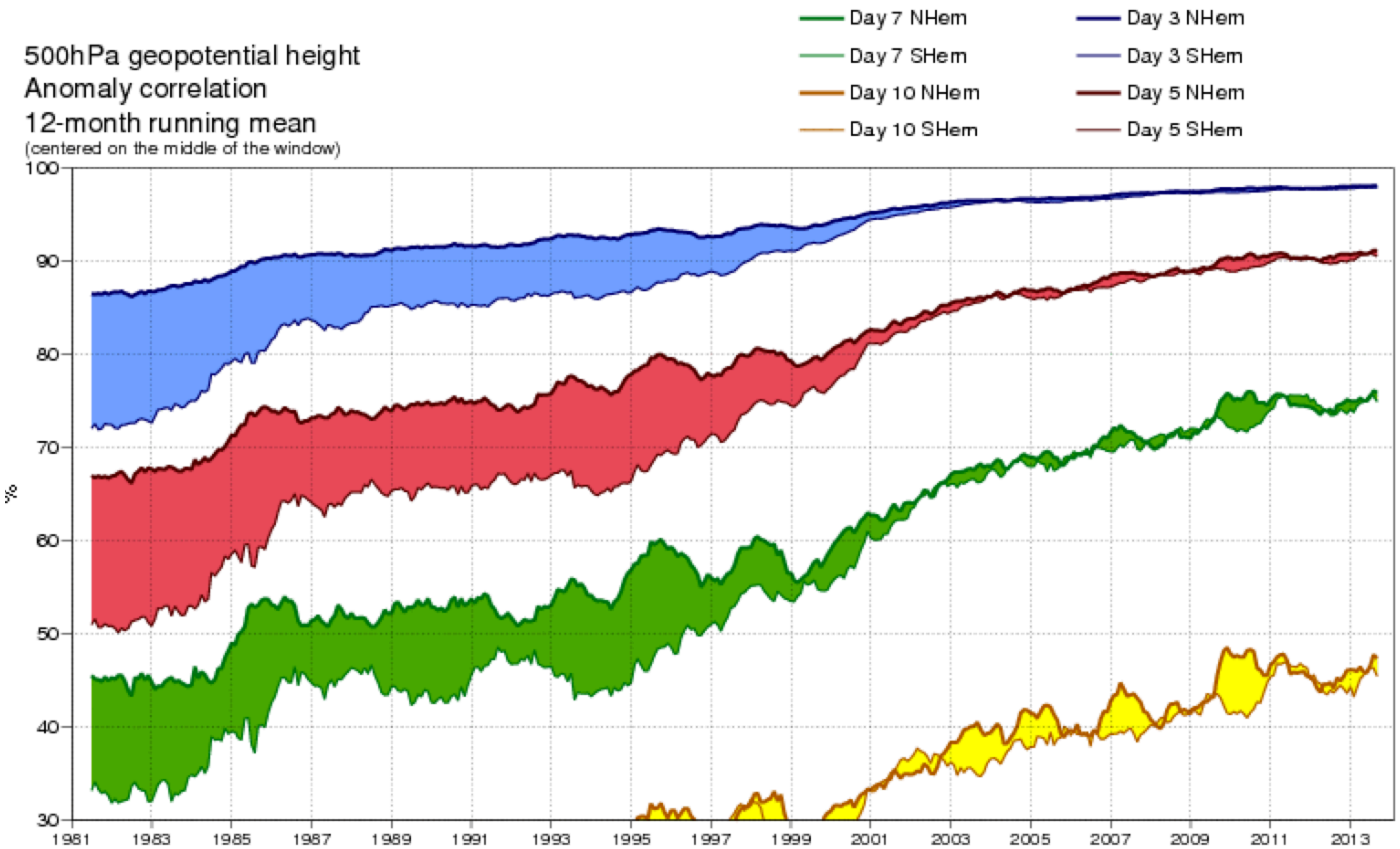

500hPa geopotential height
Anomaly correlation
12-month running mean
(centered on the middle of the window)
Day 7 NHem
Day 7 SHem
Day 10 NHem
Day 10 SHem
Day 3 NHem
Day 3 SHem
Day 5 NHem
Day 5 SHem
%
100
90
80
70
60
50
40
30
1981
1983
1985
1987
1989
1991
1993
1995
1997
1999
2001
2003
2005
2007
2009
2011
2013

Problèmes restants

- Cycle de l'eau (évaporation, condensation, influence sur le rayonnement absorbé ou émis par l'atmosphère)

- Échanges avec l'océan ou la surface continentale (chaleur, eau, quantité de mouvement, …)

- …

ECMWF

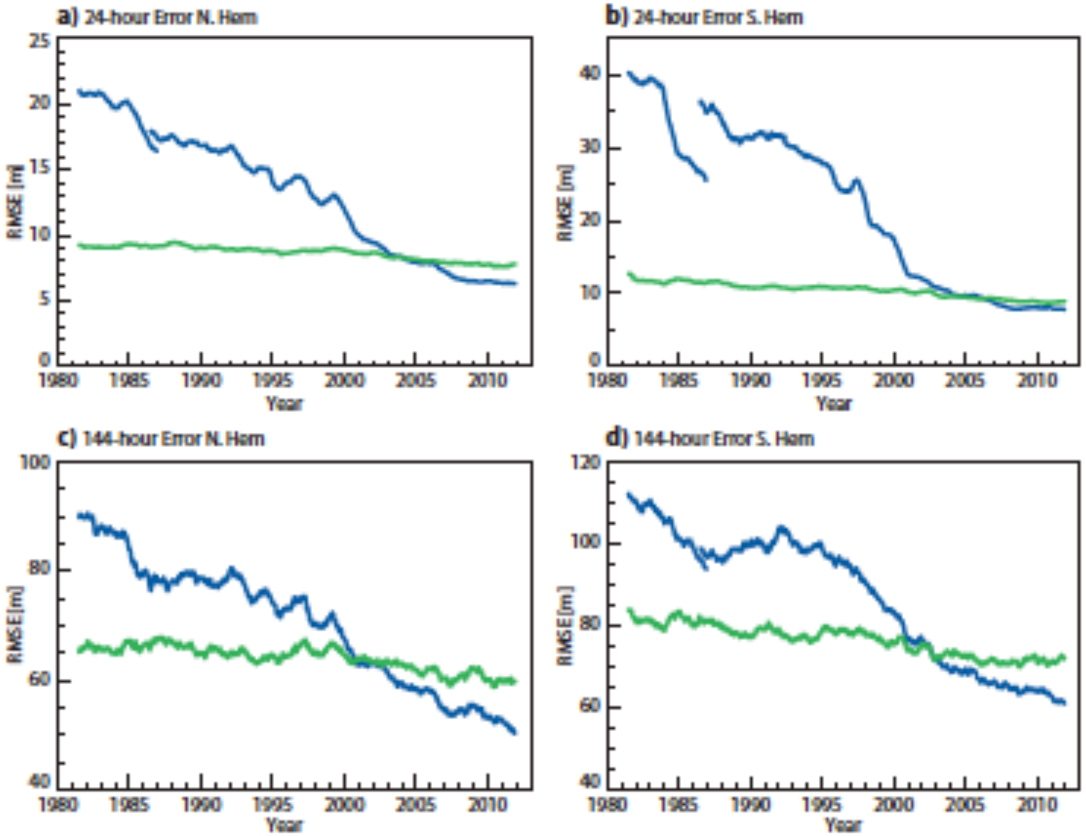

FIG. 3. Evolution of forecast errors from 1981 to 2012 for N.Hem (a and c) and S.Hem (b and d). Operational forecasts (blue) and ERA Interim (green). Note that before 1986 the operational analysis is used to verify the operational forecasts, after 1986 ERA Interim is used for the verification (with an overlap of 6 months present).

Magnusson and Källén, 2013, *Mon. Wea. Rev.*, **141**, 3142–3153

Fig. 1: Members of day 7 forecast of 500 hPa geopotential height for the ensemble originated from 25 January 1993.

Figure 6 Hurricane Katrina mean-sea-level-pressure (MSLP) analysis for 12 UTC of 29 August 2005 and t+84h high-resolution and EPS forecasts started at 00 UTC of 26 August:

1st row: *1^{st} panel: MSLP analysis for 12 UTC of 29 Aug*
2^{nd} panel: MSLP t+84h T_L511L60 forecast started at 00 UTC of 26 Aug
3^{rd} panel: MSLP t+84h EPS-control T_L255L40 forecast started at 00 UTC of 26 Aug
Other rows: 50 EPS-perturbed T_L255L40 forecast started at 00 UTC of 26 Aug.

The contour interval is 5 hPa, with shading patters for MSLP values lower than 990 hPa.

Pourquoi les météorologistes ont-ils tant de peine à prédire le temps avec quelque certitude ? Pourquoi les chutes de pluie, les tempêtes elles-mêmes nous semblent-elles arriver au hasard, de sorte que bien des gens trouvent tout naturel de prier pour avoir la pluie ou le beau temps, alors qu'ils jugeraient ridicule de demander une éclipse par une prière ?[...] un dixième de degré en plus ou en moins en un point quelconque, le cyclone éclate ici et non pas là, et il étend ses ravages sur des contrées qu'il aurait épargnées. Si on avait connu ce dixième de degré, on aurait pu le savoir d'avance, mais les observations n'étaient ni assez serrées, ni assez précises, et c'est pour cela que tout semble dû à l'intervention du hasard.

H. Poincaré, *Science et Méthode*, Paris, 1908